

Empirical Validation of Energy-Neutral Operation on Wearable Devices by MISO Beamforming of IEEE 802.11ac

Wen-Chan Shih[#], Pai H. Chou^{*†}, Wen-Tsuen Chen[#]

[#]Institute of Information Science, Academia Sinica, Taiwan

[†]Department of Computer Science, University of California, Irvine, USA

^{*}Department of Computer Science, National Tsing Hua University, Taiwan
teddyshihau@gmail.com, phchou@uci.edu, chenwt@iis.sinica.edu.tw

Abstract

We propose an approach to energy-neutral operation by Wi-Fi beamforming for wearable devices to achieve energy-neutral operation. We take advantage of the transmit beamforming feature of IEEE 802.11ac's multiple input, single output (MISO) structure to focus the transmit power to improve the transmission distance and the harvested power level. To analyze the WiFi power distribution, we design the system model of an AP's beamforming. To empirically validate our system model, we measure the wireless power of an AP in a variety of distances. Experimental results show that wearable devices with proper sampling rates can achieve an energy-neutral operation.

Categories and Subject Descriptors

H.4 [Information Systems Applications]: Miscellaneous; D.2.8 [Software Engineering]: Metrics—*complexity measures, performance measures*

General Terms

Theory

Keywords

Wi-Fi, energy scavenging, beamforming.

1 Introduction

RF energy harvesting from Wi-Fi base stations can be an important technology for a large class of devices in the Internet of Things (IoT) [4]. Particularly, deeply embedded systems may need to run on harvested power due to difficulty in battery replacement, but those that operate indoor may receive too little sunlight for photovoltaic generators. Wi-Fi base stations are now ubiquitous in homes and office environments, and they can act as a reliable source by emitting RF power in a controlled manner. Although RF energy harvesting have not been widely used due to the low level of

available power (on the order of microwatts), low-power circuit designs have advanced significantly such that it is now time to evaluate RF energy harvesting as a potentially viable energy source.

One example IoT technology that has been receiving growing attention is Bluetooth 4.0 Low Energy Technology (BLE). Its peak current consumption is 15 mA, with an average current of about 15 μ A with a duty cycle of 0.001, and a sleep current of $< 1 \mu$ A, allowing it to last for one year on a coin cell battery. This level of power consumption is starting to approach the level that can be handled by RF energy harvesting. If the level of RF energy harvesting can be increased by an order of magnitude, then it can become a viable power source for many IoT devices. While it is possible to increase power by using high-gain antennas, their large sizes would be impractical for most IoT devices, which usually must be miniature in form factor (e.g., embedded inside a coffee mug). At the same time, using directional antennas on the Wi-Fi base station, while available commercially, is not a common option in most homes due to the need for complete coverage within the home or office area.

One notable development in Wi-Fi technology is the use of beamforming in the new IEEE 802.11ac standard. Instead of a static radiation pattern of a traditional antenna, 802.11ac uses an array of antennas to achieve the effect of a focused radiation pattern dynamically in the preferential direction. This is a promising technology that has not only shown measurable gains in data rate over a range of distances but also energy efficiency. More importantly, we believe that this technology has the potential of enabling the one order of magnitude improvement needed to make RF energy harvesting practical.

We propose a space-power division multiple harvesting (SPDMH) scheme for increasing RF energy harvesting of wearable devices in the Internet of Things (IoT) and in wireless sensor networks (WSN) Existing RF energy harvesting studies focus on time division multiple harvesting through duty cycling harvesting and frequency division multiple harvesting through multiple antennas. However, they do not consider other methods to improve energy harvesting through space and power division multiple harvesting. The transmit beamforming with the Multiple-Input Single-Output (MISO) represents a promising solution to increase the RF energy harvesting.

Permission to make digital or hard copies of all or part of this work for personal or classroom use is granted without fee provided that copies are not made or distributed for profit or commercial advantage and that copies bear this notice and the full citation on the first page. To copy otherwise, to republish, to post on servers or to redistribute to lists, requires prior specific permission and/or a fee.

ENSSys'14, November 6, 2014, Memphis, TN, USA.
Copyright © 2014 ACM 978-1-4503-3189-0 ...\$10.00

To improve the harvesting power and deployment distance of the wireless sensor node, the SPDMMH scheme adopts the MISO transmit beamforming of the IEEE 802.11ac standard. As an 802.11ac-compliant access point (AP) transmits wireless signals constructively, the node with the certain sampling rate can receive more power. This means the node can execute more operations and can be deployed at longer distance from the AP. Given that the AP's primary purpose is data connection with computing devices, wearable devices can harvest Wi-Fi power of the AP opportunistically. As harvesting power can be stored in a supercapacitor of a node, a node can perform tasks as long as a supercapacitor stores a sufficient power.

In addition to supplying the operating power for IoT devices, the proposed SPDMMH technique can also provide applications such as temperature sensors deployed in smart homes or public areas with the auxiliary startup voltage for other energy harvesters such as thermoelectric ones. Together, the technology can be an important step towards energy-neutral operation of an important class of embedded systems. Experimental results show that our technique achieves better performances on the harvested power and the distance compared to conventional, non-beamforming schemes.

2 Related Work

Energy-neutral operation of wearable devices can be enhanced by energy harvesting circuits as energy harvesting circuits can harvest more energy to support perpetual operation of wearable devices. Energy harvesting devices and platforms have been proposed to improve the operating lifetime of deeply embedded systems in IoT and WSN applications. This section reviews existing energy harvesting technologies from RF sources.

RF energy harvesting has been limited to specialized systems due to the very low level of power that can be harvested. For instance, Liu et al [5] proposes prototypes with the RX power consumption of $0.54 \mu\text{W}$ using ambient RF as power source. However, this level of power is barely enough to sustain today's embedded microcontroller units (MCU) in deep-sleep mode, and any conversion such as rectifying or voltage stepping can easily incur $> 1 \mu\text{A}$ of overhead current. As a result, most of these systems operate by backscattering as the primary way to communicate with each other, similar to RFIDs.

Instead of harvesting ambient RF power, Sample et al [8] harvests the RF power emitted by a 1 MW TV tower in direct line-of-site. Results show that up to $60 \mu\text{W}$ can be harvested, which can be converted and stored to power BLE-class devices with low duty cycles. However, the system is also specialized and works primarily by backscattering; its use as a more general power supply for embedded systems still remains to be seen [10]. To provide sufficient power for existing wireless sensor nodes, the node needs to spend more time to store sufficient energy and be located close to the TV tower.

Besides RF, Bandyopadhyay et al [1] proposes parallel converters for multiple energy sources to improve the efficiency. The system performs maximum power point track-

ing (MPPT), but it works primarily on photovoltaic sources and does not include RF energy harvesting. Techniques that use of conventional Wi-Fi APs at home or public areas as the RF energy transmitter have been proposed [3, 4], but they provide insufficient level of harvestable power for most wearable devices. Several studies have been proposed to optimize beamforming vectors and power configurations [6, 7, 9]. However, they do not take a commercial Off-The-Shelf (COTS) AP into account. Moreover, our proposed SPDMMH scheme takes advantage of scavenging wireless power from existing APs opportunistically rather than dedicated or manipulating transmitters.

The MISO transmit beamforming of IEEE 802.11ac-compliant APs represents a promising technology that can bring the order of magnitude improvement needed to make it viable, but it has not been explored to date. This motivate us to adopt RF energy from Wi-Fi APs to enable energy-neutral operations of wearable devices in the IoT applications.

3 System Analysis

In SPDMMH, an AP adopts the transmit beamforming to transfer power wirelessly to the nodes over a range of distances. The distance directly impacts the available power for the nodes, while the nodes have different power requirements based on the sampling rates and communication pattern. Thus, the AP may need to take the load and distance into consideration. To improve the wireless power transfer, we adopt the MISO transmit beamforming of the IEEE 802.11ac standard. The reason for using transmit beamforming is that the IEEE 802.11ac-compliant AP's built-in multiple transmit antennas can transmit wireless power constructively and concentrate wireless power in one direction. As there can be multiple nodes that all need charging, the AP can take turns concentrating its transmit power on nodes in different directions. In this section, we investigate the proper available distance of a node, and we explore the improvements of harvesting power and distance by our proposed scheme.

3.1 Assumptions

For the purpose of analyzing the proposed SPDMMH scheme, we assume the free-space path loss, i.e., no obstacle between the AP and the node. The AP transmits wireless signals constructively. The transmitter and receiver have the full channel state information (CSI). All channels between transmit antenna and received antenna are the independent and identically distributed (i.i.d.). The scenario includes one AP and one wireless sensor node.

3.2 Available Distance of Node

Based on the available harvesting power from the IEEE 802.11ac-compliant AP with MISO transmit beamforming and the required power of the node with a variety of sampling rates, we can determine the available distance of the node.

3.2.1 Harvesting Power

To analyze the available power for harvesting from the AP, we derive the enhanced free-space path loss for MISO from the Friis transmission equation.

3.2.1.1 Path Loss for the SISO

We adopt Friis transmission equation to analyze the free-space path loss for a conventional radio system with the

single-in single-out (SISO) configuration. The equation expresses the relationship between omnidirectional antennas transmitting the same RF energy in each direction. As our proposed SPDMM adopts MISO transmit beamforming, we will augment this equation with directionality later. From Friis transmission equation in Eqn. (1), we can determine the signal power at the node's antenna from the AP with the given distance. The available power of the node's receiving antenna P_{rx}^{ant} with free-space path loss for SISO is given by

$$P_{rx}^{ant} = P_{tx}^{ant} A_{gain}^{ary} G_{tx}^{ant} G_{rx}^{ant} \left(\frac{\lambda}{4\pi D} \right)^2 \frac{1}{\chi_{fad}^{sha}}, \quad (1)$$

where the *array gain* A_{gain}^{ary} is given by

$$A_{gain}^{ary} = 10 \log_{10}(N_{tx}). \quad (2)$$

where N_{tx} is the *number of transmit antennas*. We only consider the mobility of a wearable device, but we do not take the actual Body Area Network (BAN) scenario into account, such as channel model or loss. This will be our future work.

To compare SISO and MISO configuration fairly, the SISO configuration adopts the same N_{tx} and total transmit power. The constructive transmission with given N_{tx} linearly scales the voltage on the transmitter antennas to $N_{tx}V$. The output power of the transmission antennas is derived by the square of the constructive voltage, i.e., N_{tx}^2V . As the N_{tx} transmits N_{tx} times transmit power, the A_{gain}^{ary} presents the additional gain of $N_{tx}^2/N_{tx} = N_{tx}$. Thus, the A_{gain}^{ary} is derived by $10 \log_{10}(N_{tx})$. The P_{tx}^{ant} is the output power of the AP's transmitting antenna, G_{tx}^{ant} is the antenna gain of the AP's transmitting antenna, G_{rx}^{ant} is the antenna gain of the node's receiving antenna, λ is the wavelength, D is the distance between transmitting and receiving antennas, and χ_{fad}^{sha} is the shadow fading [2]. The value of the P_{tx}^{ant} is large than the value of the P_{rx}^{ant} as the free-space path loss. Thus, the ratio of P_{rx}^{ant} and P_{tx}^{ant} is less than 1.

3.2.1.2 Enhanced Path Loss for the MISO

To consider the transmit beamforming with directional antenna effect, we enhance the Friis transmission equation by adding the *beamforming gain* B_{gain}^{bf} . We employ the B_{gain}^{bf} into the Friis transmission equation in Eqn. (1) to enhance the analysis capability for the MISO. The available power of the node's receiving antenna $P_{rx.en}^{ant}$ with free-space path loss and the certain N_{tx} of the AP is given by

$$P_{rx.en}^{ant} = P_{tx}^{ant} B_{gain}^{bf} A_{gain}^{ary} G_{tx}^{ant} G_{rx}^{ant} \left(\frac{\lambda}{4\pi D} \right)^2 \frac{1}{\chi_{fad}^{sha}}, \quad (3)$$

where B_{gain}^{bf} is given by

$$B_{gain}^{bf} = 2\pi / \theta_{bf}^{ml}, \quad (4)$$

where θ_{bf}^{ml} is the main lobe degree of the beamforming.

Wireless energy is distributed in two parts: main lobe and back lobe. As the main lobe occupies most of wireless energy, we only take main energy beam into account. Therefore, Eqn. (4) does not consider the back lobe of the beamforming. If Eqn. (4) considers a back lobe portion of the

beamforming, then it will be more realistic. This will be our future work.

3.2.2 Required Power of the Node

The required power of the node depends on the *sampling rate* R_s and power consumption of the node. From the data sheet of a popular chip for IoT, the TI CC2540 integrated MCU and Bluetooth Low Energy RF, we can find empirical data such as the active current I_{node}^{idle} of 19.6 mA and the idle current I_{node}^{active} of 0.4 μ A in power mode 3. The operating voltage V_{node} is 2.2 V. Given the sampling rate R_s , the average power consumption of the node P_{node}^{avg} is given by

$$P_{node}^{avg} = V_{node} I_{node}^{avg}, \quad (5)$$

where I_{node}^{avg} is the *average current of the node* that is given by

$$I_{node}^{avg} = I_{node}^{active} R_s + I_{node}^{idle} (1 - R_s). \quad (6)$$

The value of the sampling rate R_s depends on the requirement of the application. For example, emergency sensing such as fire alarm requires faster response, but non-emergency application such as temperature sensing may be much less stringent.

Improvement of harvesting power from the proposed scheme can be calculated as follows. Given the *frequency* $Freq$, the P_{tx}^{ant} , and the D , the harvesting power improvement P_{imp}^{har} from Eqn. (1) and (3) is given by

$$P_{imp}^{har} = P_{rx.en}^{ant}(Freq, D) - P_{rx}^{ant}(Freq, D). \quad (7)$$

Given the frequency $Freq$ and the available receiving power P_{ava} , the distance improvement D_{imp} is given by

$$D_{imp} = D_{en}(P_{ava}, Freq) - D(P_{ava}, Freq), \quad (8)$$

4 Performance Evaluation

In this section, we first describe the parameters of system configuration for simulation. To evaluate the performance of our scheme, we determine the available distances based on the available power from the AP and power requirement of the node. Base on the improvement of available distances, we explore the extra power harvesting at given distance and extra distance at given power. We build the system model by Python programming language and plot simulation results by Matplotlib to expose the salient characteristics. From the available power at receiver's antenna, P_{rx}^{ant} and $P_{rx.en}^{ant}$, and the required power of a node P_{node}^{avg} , we calculate the available distance of a node.

4.1 Configuration

We adopt empirical data from data sheets for simulation. Table 1 summarizes the simulation parameters for the available distance and improvements. The scenario includes one AP with the number of antennas N_{tx} and one node at a variety of distances.

4.2 Available Distances of Node

To determine available distances of the node, we evaluate the harvesting power from the AP's transmit beamforming and the power requirement of the node. Fig. 1 shows the harvesting power, the required power, and the available distance. The SR denotes the sampling rate. We observe that the

Table 1: Simulation parameters for the available distance and improvements

Description	Parameter	Value	Units
No. of APs	N_{ap}	1	set
No. of transmit antennas	N_{tx}	4	set
Frequency of AP	F_{ap}	2.4, 5	GHz
Transmit power of AP	P_{ap}	23.45	dBm
Antenna gain of AP	G_{tx}	6	dBi
Antenna gain of node	G_{rx}	5	dBi
No. of node	N_n	1	set
Idle current of node	I_{node}^{idle}	0.4	μA
Active current of node	I_{node}^{active}	19.6	mA
Voltage of node	V_{node}	2.2	V

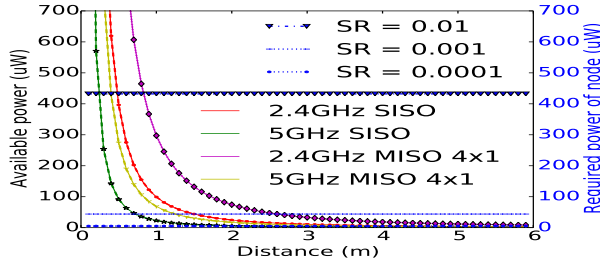


Figure 1: Available distance based on harvesting and required powers

MISO scheme offers higher flexibility for a node. The flexibility can increase energy of a node to do more tasks and also bring users more mobility. The transmit beamforming power decreases by free-space path loss when the distance between the AP and the node increases. The free-space path loss decreases when the frequency decreases. We use the transmit beamforming of 4×1 MISO to find the available distance. We adopt a variety of sampling rates to reduce the power consumption of the node. The sampling rates are 10^{-2} , 10^{-3} , and 10^{-4} in the simulation.

4.3 Harvesting Power Improvement

Fig. 2 shows the harvesting power improvement by the proposed SPDMH. We examine that array gain increases when number of antenna of the AP N_{tx} increases. Due to the rapid increment on extra power harvesting, our scheme in the 2.4 GHz band can provide higher harvestable power for a node.

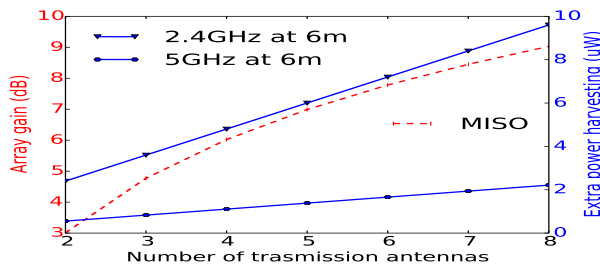


Figure 2: Harvesting improvement by the proposed SPDMH

Table 2: Improvements on available power and distance

θ_{bf}^m	45°	120°
P_{har}^{imp}	87.5 %	66.67 %
D_{imp}	64.64 %	42.26 %

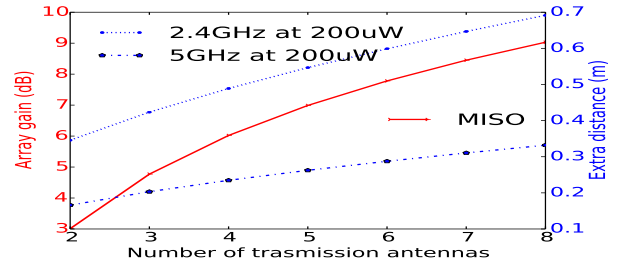


Figure 3: Distance improvement by the proposed SPDMH

4.4 Distance Improvement

Fig. 3 shows the distance improvement by the proposed SPDMH. From the results, we observe that when the array gain increases, harvesting power extends the available distance of a node. Compared to 2.4 GHz, 5 GHz has a slow increment on the extra distance, and we conclude that 2.4 GHz can obtain a longer available distance for a node.

Table2 summarizes improvements on available power and distance. The improvements are independent of the number of antennas and location of wearable devices. Fig. 4 shows that the extra harvestable power is a function of the distance and the number of antennas. We observe that lower frequency and more antennas result in more extra harvestable power.

5 Empirical Validation

We perform proof-of-concept experimental validation of the MISO beamforming of IEEE 802.11ac. The purpose of the experiments is to validate the system model and empirically evaluate the available power of a commercial off-the-shelf (COTS) AP. In this section, we describe the experimental setup and scenario, with a discussion on the results and the system model.

5.1 Experimental Setup

Fig. 5a shows the floor map for our experimental setup at the communication SOC Lab in National Tsing Hua Uni-

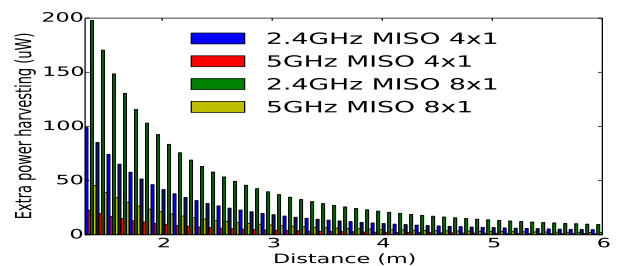


Figure 4: Harvesting improvement depends on distance and the number of antennas

versity, Hsinchu, Taiwan. To measure cable loss and available power of the monitor antenna at a certain distance, we employ a Rohde & Schwarz FSU spectrum analyzer with a frequency range of 20 Hz to 8 GHz and a Rohde & Schwarz SMIQ06B signal generator with a frequency range of 300 kHz to 6.4 GHz. The Apple AirPort Extreme (AE) has been chosen to be the Wi-Fi energy source of the MISO Beamforming of the IEEE 802.11ac. We use Apple's AirPort Utility to configure parameters of the AE from a MacBook Air (MA). Another reason to choose the AE is the available online resources for modifying the behavior of the AE. For a variety of experimental scenarios, we employ two Apple MAs, one with the IEEE 802.11ac-compliance (MAac) and the other one without the IEEE 802.11ac-compliance, and we attached an ASUS USB-AC56 USB Wi-Fi dongle (UD) with the IEEE 802.11ac-compliance (MAud). To measure the available power at a variety of distances, we employ a CERIO ANT-0608RS omnidirectional dual band antenna with antenna gains of 6 dBi for 2.4 GHz and 8 dBi for 5 GHz as the monitoring antenna (Mant). We configure the frequency of the AE to the channel 149 of 5.745 GHz. To measure available power of the Mant, we set up Rohde & Schwarz spectrum analyzer at the same frequency. In terms of cable losses, we measure cable losses by a Rohde & Schwarz signal generator and a Rohde & Schwarz spectrum analyzer at the frequency of 5.745 GHz. Two cable losses are -4.33 dBm and -13.67 dBm at 5.745 GHz for 1×1.5 m and 5×1 m, respectively.

5.2 Scenarios

Our experiments were conducted in the corridor and in the chamber. The corridor is marked as 1 in Fig. 5a and Fig. 5b, and there are some metallic materials around the corridor. The length of the corridor is about 5 m. The RF anechoic chamber, marked as 2 in Fig. 5a and Fig. 5c, is about $2 \times 2 \times 2 m^3$ in volume. Inside of the chamber is covered by Home Sun absorbing foam pyramid HS-P3 with an absorption value of 28 dB at 5 GHz. The experimental scenarios can be categorized into three cases.

5.2.1 Case 1 : Moving AE in the Corridor

In this case, we explore how much available power nearby a laptop when the laptop is downloading a large file of about 20 GB while the AP is moving away. We fix positions of MAac and Mant. We arrange the MAac on the Rx position and Mant on the Ant position in Fig. 5a. We only move AE by 20 cm each time and measure the available power on the Mant. The AE is moved from 10 cm away from Mant to the Tx position in Fig. 5a. The distance of MAac and Mant is about 20 cm. The maximum distance of Mant to AE is about 5 m as the Lab's space limit. The Mant is held by a tripod. The MAac and AE are on chairs. The height of MAac, Mant, and AE are about 60 cm from the ground.

5.2.2 Case 2 : Moving Monitoring Antenna in the Corridor

To investigate the available power at the certain distance away from the AP between fixed laptop and AP when the laptop is downloading a large file of about 20 GB. We fix the positions of MAud and AE at the Rx and Tx spots in Fig. 5a, respectively. We only move Mant from 10 cm away from AE

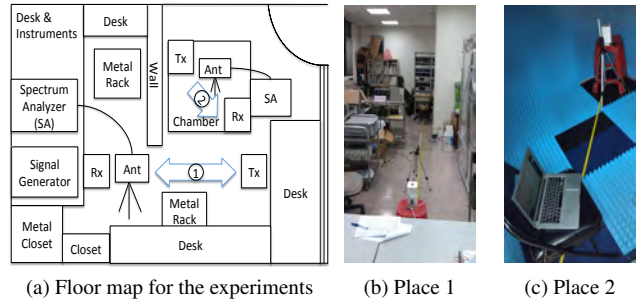


Figure 5: Floor map and experimental places

to the Rx position in Fig. 5a. The moving direction of Mant is opposite to the AE in case 1. In terms of parameters relevant to the transmit power of AE, we configure the country pick-up list to Taiwan (TW) and Guam in wireless option of the AirPort Utility to investigate the respective transmit power control.

5.2.3 Case 3 : Moving Monitoring Antenna in the Chamber

To reduce interference from RF reflections by metal materials around the corridor, we arrange experiment into a chamber. As the chamber is space-constrained, the available moving distance of Mant is about 1.3 m. The only difference between case 3 and case 2 is a shorter moving distance in the chamber. In this case, we control the transmit power of AE by country configurations of TW and Guam in case 2.

5.3 Discussions on Empirical Results and System Model

We discuss the difference between empirical results and system model with empirical configurations. The upper bound of available power can be calculated by system model with empirical configurations. To enhance the transmit power, we use the AirPort Utility to control the transmit power. We observe the reflections and salient characteristics of available power relevant to environment and configuration of AE.

5.3.1 Upper Bound of Available Power

Fig. 6 shows empirical available power in a variety of distances. The first curve shows the simulation results of the system model. The second and third curves respectively use the case-1 and case-3 scenarios with the TW configuration, while The fourth and fifth curves respectively use the case-2 and case-3 scenarios with Guam configuration. As the system model based on free-space path loss and shadow fading, the simulation results of the system model can be considered the upper bound of available power. The MISO upper bound is calculated by Eqn. (3) with the standard deviation for shadow fading of the mean μ of 10.6 dB and the standard deviation σ of 2.3 dB [2]. In the calculation, the transmit power of 28.01 dBm refers to a certificate from the National Communications Commission, Taiwan, for Apple Airport Extreme A1521 at 5 GHz. We also apply parameters such as three antennas of the AP and empirical beamforming angle of 120° in the calculation.

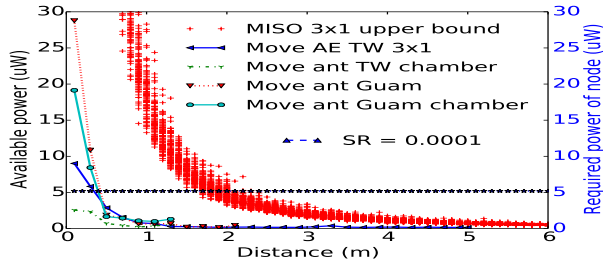


Figure 6: Empirical experimental results

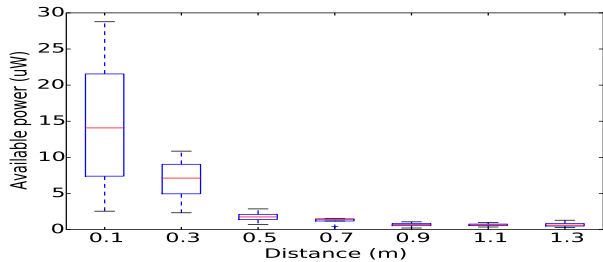


Figure 7: Characterizations of experiments

5.3.2 Transmit Power Control

To adjust the transmit power of the AP, we employ the AirPort Utility 5.6.1 for Windows as the AirPort Utility 6.3.2 for MacOS X does not support transmit power configuration. The country configuration of Guam in the AirPort Utility has a higher transmit power than TW as the transmit power depends on country regulation. This configuration can achieve an improvement of up to $17 \mu\text{W}$ that can bring more power to a wearable device.

5.3.3 Impact of Reflections

The interesting point is that the available power measured in the chamber is not higher than one in the corridor, even though there is less interference in the chamber. Two reasons can explain this. One is that some reflections from metal materials around the corridor are constructive. The other reason is the AE has an internal power control. If the client distance is farther, then AE increases its power to maintain the client's receiver signal strength at the certain level. As the chamber has a shorter distance than the corridor, the transmit power of AE is lower by about $6 \mu\text{W}$.

5.3.4 Characterization of Available Power

Fig. 7 shows characterizations of available power in a variety of distances with all scenarios. We observe that closer distances have larger variances in available power due to configurable transmit power, fewer reflections in the chamber, and more or less of transmit power from an AP. Over longer distances, the available powers are more consistent.

Based on above discussion, a BLE-based node can make use of a patch antenna and a rectifier to harvest and store Wi-Fi energy into a supercapacitor. With the proper sampling rate, such a node is expected to be able to achieve an energy-neutral operation.

6 Conclusions

We propose energy-neutral operation using transmit beamforming to enhance wireless energy harvesting for low power wearable devices. To analyze the performance of the transmit beamforming, we present the system model to investigate the available harvesting power and distance improvements. From empirical experimental results, our system model is consistent with the available harvesting power from an AP. Low power wearable devices with proper sampling rates can achieve an energy-neutral operation. Therefore, we believe our work represents a first step towards making RF energy harvesting from Wi-Fi a viable option for IoT devices.

7 Acknowledgments

The authors thank Prof. Jen-Ming Wu and his student Mr. Kai-Chieh Tang in the communication SOC Lab, and Mr. Yung-Shun Wang, National Tsing Hua University, Hsinchu, Taiwan, as well as, Prof. Shyh-Jong Chung, National Chiao Tung University, Hsinchu, and Mr. Shi-Sheng Sun, National Taiwan University, Taipei, Taiwan for for high frequency instruments support and discussion. This research is funded in part by the Thematic Research Program of Academia Sinica under Grant Number 23-24 and Intel-NTU Connected Context Computing Center: M2M-TRAC.

8 References

- [1] S. Bandyopadhyay and A. Chandrakasan. Platform architecture for solar, thermal, and vibration energy combining with mppt and single inductor. *IEEE Journal of Solid-State Circuits*, 47(9):2199–2215, 2012.
- [2] V. Erceg, L. Greenstein, S. Tjandra, S. Parkoff, A. Gupta, B. Kulic, A. Julius, and R. Bianchi. An empirically based path loss model for wireless channels in suburban environments. *IEEE Journal on Selected Areas in Communications*, 17(7):1205–1211, Jul 1999.
- [3] S. Gollakota, M. Reynolds, J. Smith, and D. Wetherall. The emergence of RF-powered computing. *Computer*, 47(1):32–39, Jan 2014.
- [4] B. Kelllogg, A. Parks, S. Gollakota, J. R. Smith, and D. Wetherall. Wi-Fi Backscatter: Internet connectivity for RF-powered devices. In *Proceedings of ACM SIGCOMM*, August 2014.
- [5] V. Liu, A. Parks, V. Talla, S. Gollakota, D. Wetherall, and J. R. Smith. Ambient backscatter: wireless communication out of thin air. In *Proceedings of the ACM SIGCOMM 2013 conference on SIGCOMM, SIGCOMM '13*, pages 39–50, New York, NY, USA, 2013. ACM.
- [6] R. Morsi, D. S. Michalopoulos, and R. Schober. Multi-user scheduling schemes for simultaneous wireless information and power transfer. In *Proceedings of IEEE International Conference on Communications, ICC 2014, Sydney, Australia, June 10-14, 2014*, pages 4994–4999, 2014.
- [7] D. W. K. Ng, R. Schober, and H. M. Alnuweiri. Secure layered transmission in multicast systems with wireless information and power transfer. In *Proceedings of IEEE International Conference on Communications, ICC 2014, Sydney, Australia, June 10-14, 2014*, pages 5389–5395, 2014.
- [8] A. Sample and J. Smith. Experimental results with two wireless power transfer systems. In *Proceedings of IEEE Radio and Wireless Symposium (RWS)*, pages 16–18, 2009.
- [9] S. Timotheou, I. Krikidis, G. Zheng, and B. Ottersten. Beamforming for MISO interference channels with qos and RF energy transfer. *IEEE Transactions on Wireless Communications*, 13(5):2646–2658, May 2014.
- [10] Y.-H. Tu, Y.-C. Lee, Y.-W. Tsai, P. H. Chou, and T.-C. Chien. Eco-Cast: Interactive, object-oriented macroprogramming for networks of ultra-compact wireless sensor nodes. In *Proceedings of the 10th International Conference on Information Processing in Sensor Networks (IPSN)*, pages 113–114, 2011.